Side-Chain Liquid-Crystalline Polyoxetanes with a Spacer-Separated Azobenzene Moiety. II. Preparation and Characterization of Polyoxetanes Derived from 4-(4-Alkoxyphenylazo)phenyl 4-[7-(3-Methyl-3-oxetanyl)-1,6-dioxaheptyl]-benzoates

Hiroshi Ogawa, Tetsuya Hosomi, Toshiaki Kosaka, Shigeyoshi Kanoh, Akihiko Ueyama,† and Masatoshi Motoi*

Department of Chemistry and Chemical Engineering, Faculty of Engineering, Kanazawa University, 2-40-20 Kodatsuno, Kanazawa 920

†New Materials Development Department, Industrial Technology Center of Fukui Prefecture, 61 Kawaiwashizuka, Fukui 910

(Received June 27, 1996)

A series of polyoxetanes were prepared by the cationic ring-opening polymerization of 4-(4-alkoxyphenylazo)phenyl 4-[7-(3-methyl-3-oxetanyl)-1,6-dioxaheptyl]benzoates using 0.08 molar amount of $THF{\cdot}BF_3$ in dichloromethane at 20 to 30 °C. Although the product polymers indicated GPC-average molecular weights of around 9000 to 23000, in most cases, they did not have an unimodal molecular weight dispersity. The liquid-crystalline mesophases of the polymers were examined by differential scanning calorimetry and polarized optical microscopy; these textures were observed due to nematic and/or smectic mesophases over a wide temperature range from about 250 °C to room temperature. The benzoate moiety, the longer *p*-substituted alkoxy tails, and the oxetane main chain play important roles in maintaining highly ordered, stable mesophases.

Our investigation was carried out in order to find useful polyoxetane-based functional polymers, since we consider that their functioning ability is favored by several desired properties of the polyoxetane matrices.[1—4] Thus, from the viewpoint of applying polyoxetane to the main chain of side-chain liquid-crystalline polymers, our preceding paper reported on the preparation and characterization of polyoxetanes, poly(**1**)s, derived from oxetanes **1a**, **1b**, **1e**, **1i**, and so on.[5] These polymers anchored only pendant azobenzene cores modified with spacers and tails of differing lengths at the *p*- and *p*′-positions; in this text, henceforth, the *o*-, *m*-, and *p*-positions of the azobenzene are conveniently given for the benzene ring linked to the spacer and the *o*′-, *m*′-, and *p*′-positions for that linked to the tail, as shown in Scheme 1, although the IUPAC nomenclatures are also used for these substances.

To date, several reports concerning polyoxetane- and polyoxirane-based side-chain liquid-crystalline polymers have been made by other authors. These polyethers were obtained by a cationic ring-opening polymerization of the corresponding monomers with pendant spacer-separated mesogns, e.g., 4′-cyano-, 4′-fluoro-, and 4′-alkoxy-4-biphenylyls, 4-spacer-substituted phenyl *trans*-4-alkyl-1-cyclohexanecarboxylates, and 2,5-bis(4-substituted benzoyloxy)benzoyls.[6—9] These mesogens allowed the production of a variety of optical textures. Polyoxiranes carrying the pendant mesogen of (4′-cyano-4-biphenylyloxy)methyl were also prepared by a polymer reaction of poly(epichlorohydrin)s having differing molecular weights with the corresponding 4-biphenylol. The thus-obtained pendant mesogens formed an enantiotropically mematic phase in spite of being linked to the polymer backbone through a short spacer, $-CH_2O-$, with low flexibility. This fact was ascribed to the contribution of the flexibility of the ether backbone to the liquid-crystalline ordering of the pendant mesogens.[10]

In the present report concerning the preparation and characterization of side-chain liquid-crystalline polyoxetanes, 4-spacer-substituted benzoates were chosen as a part of the mesogenic core, as shown in the pendant chains of the polymers, poly(**2**)s, derived from oxetanes **2a**—**2k**. Compared with the structure of poly(**1**)s, the structure of poly(**2**)s serves to prove the effect of the benzoic ester moiety on the liquid-crystalline properties of the polyoxetanes. In general, it is known that the benzoic ester moiety is a polar segment which is often required to organize mesogenic groups in a liquid-crystalline state. In this study, the benzoic ester of poly(**2**)s was found to be an important mesogenic segment in liquid-crystalline polymers, showing their mesophases over a wide temperature range on differential scanning calorimetry (DSC) and polarized optical microscopy (POM). Polymers

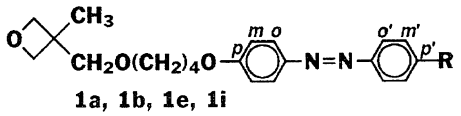

1a, 1b, 1e, 1i

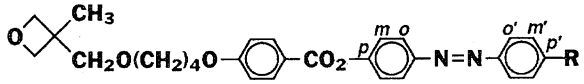

2a—2k

	R		R
1a, 2a	H	2g	OC_6H_{13}
1b, 2b	OCH_3	2h	OC_7H_{15}
2c	OC_2H_5	1i, 2i	OC_8H_{17}
2d	OC_3H_7	2j	$OC_{10}H_{21}$
1e, 2e	OC_4H_9	2k	$OC_{12}H_{25}$
2f	OC_5H_{11}		

3 : X= 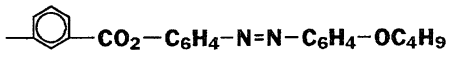

4 : X= 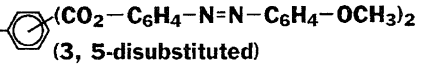

5 : X= —C_6H_4—CH_2CO_2—C_6H_4—N=N—C_6H_4—OC_4H_9

6 : X= —C_6H_4—CO_2—C_6H_4—OC_8H_{17}

Scheme 1. Oxetane monomers used in the present study. C_6H_4 presents an 1,4-phenylene group.

of **3**—**6** were also prepared in order to examine the suitability for the benzoate structure in liquid-crystalline polymers, compared with poly(**2**)s.

Results and Discussion

Oxetanes and Their Polymers. A synthetic route is shown in Scheme 2 for preparing oxetanes **2a**—**2k** and their polymers. The spacer-separated bromine atom of oxetane **7** was replaced by a phenoxide derived from ethyl 4-hydroxybenzoate with anhydrous K_2CO_3 in *N*,*N*-dimethylformamide (DMF) to give the corresponding benzoate **8**. This ester residue was readily hydrolyzed with 2 mol dm^{-3} NaOH in methanol under reflux without any side reactions of the oxetane ring. The resultant benzoic acid of **9** was converted to the desired oxetane monomers **2a**—**2k** by an ester-condensation reaction with *p*-phenylazophenols in the presence of *N*,*N*′-dicyclohexylcarbodiimide (DCC) and 4-dimethylaminopyridine (DMAP). Oxetanes **3**—**6** were similarly obtained using the corresponding mono- and dicarboxylic ethyl esters in place of ethyl 4-hydroxybenzoate. After purification by recrystallization from appropriate solvents, these oxetane monomers were subjected to cationic ring-opening polymerization with a tetrahydrofuran–trifluoroboran (1/1) complex (THF·BF_3) as an initiator. The results are summarized in Table 1. Dichloromethane (DCM) or toluene or their mixture was chosen as a polymerization solvent, although the oxetane monomers used in this study had a tendency to dissolve somewhat readily in DCM, rather than in toluene. The polymerization temperature was set at room temperature (20 to 30 °C), since the monomers deposited below 0 °C, even in DCM. The raw product polymers were reprecipitated two or three times from DCM to methanol to give polyoxetanes poly(**2a**)—poly(**2k**) in fairly good yields.

The molecular weights of the polymers were estimated by gel-permeation chromatography (GPC) relative to the polystyrene standards, and are also listed in Table 1. The polymers exhibited GPC-average molecular weights (M_{gpc}) of around 9000 to 23000 in spite of using large amounts, such as 0.08 to 0.25 molar amount, of THF·BF_3 to the monomer; 5×10^{-3} to 1×10^{-2} molar amount of THF·BF_3 is used in the ordinary polymerization procedure of oxetanes. An increased amount of THF·BF_3 was required to obtain the polymers in fairly high yields, since the azobenzene moiety tended to hinder the initiation reaction when using small amounts of BF_3, although the ester moiety did not interrupt the initiation with an ordinary amount of BF_3.[11] GPC chromatograms of poly(**2b**) and poly(**2e**) are exempli-

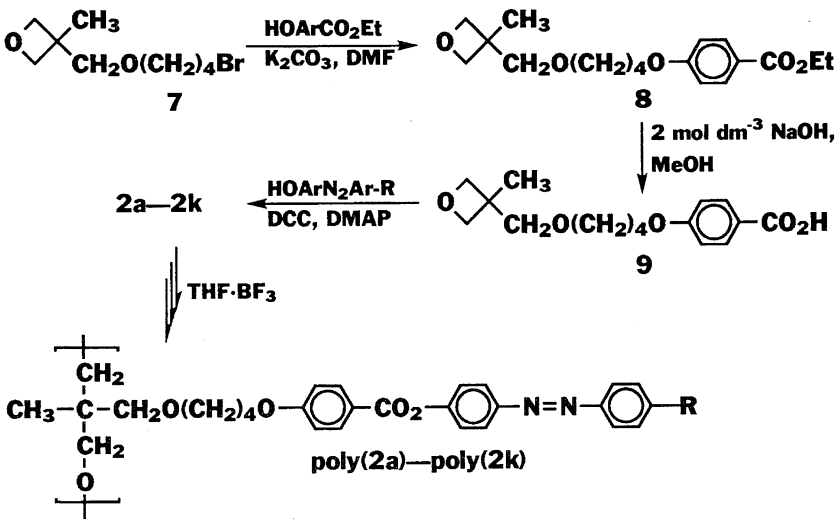

Scheme 2. A synthetic route of oxetanes and their polymers.

Table 1. Preparation of Polyoxetanes by Cationic Ring-Opening Polymerization[a)]

Polymer	$[M]_o$[b)] / mol dm^{-3}	BF_3 molar amount	Solvent (Volume ratio)	Yield[c)] / %	$10^{-4} \times M_{gpc}$[d)]
Poly(**2a**)	0.9	0.08	T	79	2.65, 1.34, 0.17
Poly(**2b**)	0.9	0.08	T	79	2.92, 1.59, 0.28
Poly(**2b**)-1	2.3	0.05	T	88	3.00, 1.50, 0.23
Poly(**2b**)-2	1.0	0.08	DCM	88	(2.7), 1.35, 0.25
Poly(**2c**)	0.4	0.08	DCM	85	0.97, 0.20
Poly(**2d**)	0.6	0.08	DCM	91	1.13, 0.22
Poly(**2e**)	0.6	0.08	DCM+T (1 : 2)	89	2.27, 1.13, 0.24
Poly(**2e**)-1	0.3	0.08	T	55	3.00, 1.15, 0.27
Poly(**2e**)-2	0.5	0.08	DCM	85	2.36, 1.31, 0.27
Poly(**2e**)-3	0.5	0.15	DCM	91	(2.2), 1.15, 0.27
Poly(**2e**)-4	0.5	0.25	DCM	90	2.19, 1.23, 0.27
Poly(**2f**)	0.6	0.08	DCM+T (1 : 2)	97	2.31, 1.17, 0.27
Poly(**2g**)	0.5	0.08	DCM	94	2.32, 1.26, 0.29
Poly(**2h**)	1.0	0.08	DCM	97	2.73, 0.31
Poly(**2i**)	0.7	0.08	T	98	2.84, 1.18, 0.35
Poly(**2j**)	0.8	0.08	DCM	92	2.65, 1.49, 0.46
Poly(**2k**)	0.5	0.08	DCM+T (1 : 2)	93	2.57, 1.22, 0.43
Poly(**3**)	0.6	0.08	T	79	0.98, 0.24
Poly(**4**)	0.7	0.08	DCM	91	2.08, 1.13, 0.31
Poly(**5**)	0.2	0.08	DCM+T (2 : 3)	63	0.74, 0.27
Poly(**6**)	0.6	0.02	DCM	90	1.12, 0.22

a) Carried out using 0.02—0.25 molar amount of THF·BF_3 in dichloromethane (DCM) or toluene (T) or their mixture at 20—30 °C for 50 h. b) Initial monomer concentration. c) For a methanol-insoluble fraction. d) M_{gpc} values in parentheses are given for shoulder peaks.

fied in Figs. 1 and 2 to illustrate the results of the GPC of the polyoxetanes listed in Table 1. The molecular-weight dispersity (MWD) curves of the main fractions of poly(**2**)s were dimodal or more multimodal, also suggesting the generation of more than two types of active propagating species in the BF_3-initiated cationic ring-opening polymerization of **2a**—**2k**, as discussed in a previous paper concerning the preparation of poly(**1**)s.[5)] The peaks at molecular weights of around 2000 to 3000 were ascribed to those of the oligomers not removed from the main fraction by repeated reprecipitation of the raw product polymers. For each polymer shown in Figs. 1 and 2, two main peaks were observed at around M_{gpc} 22000—30000 and 11000—16000, and the amount of the lower-molecular-weight fraction tended to increase relative to that of the higher-molecular-weight fraction when using an increased amount of THF·BF_3 [(a) and (b) in Fig. 1 and (c), (d), and (e) in Fig. 2]. This tendency was also observed when DCM was used as a polymerization solvent in place of toluene [(b) and (c) in Fig. 1 and (a), (b), and (c) in Fig. 2]. Thus, the amount of THF·BF_3 and the polarity of the solvent influenced the character of the active propagating species, which govern not only the polymerization mechanism and kinetics of oxetanes, but also the M_{gpc} and MWD of the product polymer. It is an interesting problem as to whether these active propagating species can control stereoregularly the propagation reaction of oxetanes, resulting in the production of an isotactic or syndiotactic polyoxetane. However, although this report does not deal with such a problem, the formation of atactic polymers was reported for the ring-opening polymerization of several oxetanes having non-mesogenic groups at the C-2 or C-3 position.[12—15)]

Figure 3 shows the ^{1}H NMR spectra of **2k** and poly(**2k**), respectively, for examples of the oxetane monomers and their polymers. These protons, H^a to H^o, were assigned to the corresponding signals, (a) to (o), according to the procedure given in our previous report.[5)] The chemical shifts and patterns of the signals of poly(**2k**) resemble those of monomer **2k**, except for the signals of the methyl (H^c) and methylene protons (H^e and H^i). The protons of the methyl and methylene groups adjacent to the quaternary carbon atom of poly(**1**)s also resonated at the ordinary chemical shifts lower than those of the corresponding protons of the oxetane ring. The IR bands of the cyclic ether were observed at 980 and 840 cm^{-1} in the IR spectrum of **2k**, but not in that of poly(**2k**). The structures of poly(**2a**) to poly(**2k**) were also confirmed based on their elemental-analysis values, which agreed approximately with the calculated ones (Table 2).

DSC and POM of Polyoxetanes. The liquid-crystalline properties of the polyoxetanes were examined by their DSC and POM. Figures 4 and 5 show the DSC traces for poly(**2b**) and poly(**2i**), respectively. The DSC curves, recorded repeatedly after the first cooling process followed by a second heating process, were similar to the corresponding DSC curves observed for these processes. The endo- or exothermic peak at the highest temperature of each DSC trace is due to the isotropic phase transition upon heating or cooling. At these isotropic phase-transition temperatures (T_i) the isotropic phase was confirmed based on the POM texture.

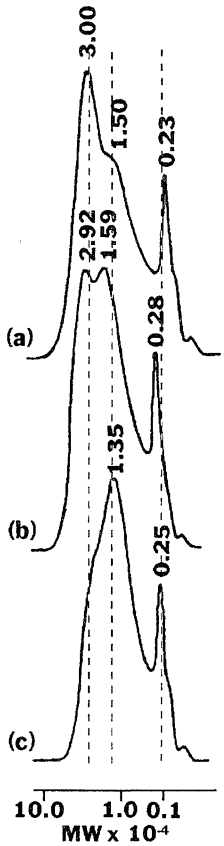

Fig. 1. GPC chromatograms of poly(**2b**)s obtained using the following BF_3 amount ($\times 10^{-2}$ molar amount) and solvent: (a) 5, toluene; (b) 8, toluene; (c) 8, DCM. Figures at peak tops indicate molecular weights ($\times 10^{-4}$) estimated from those of polystyrene standards.

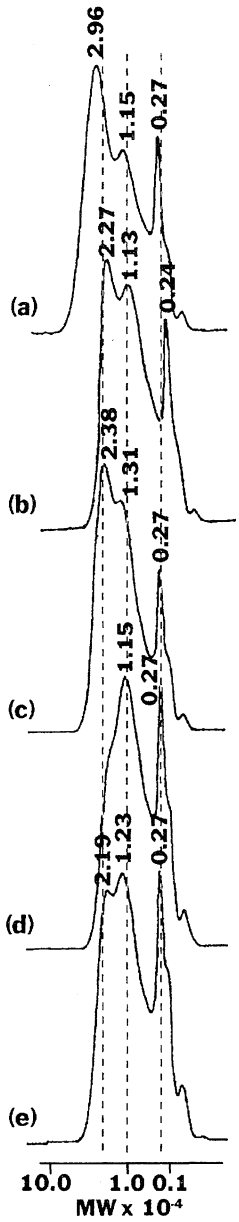

Fig. 2. GPC chromatograms of poly(**2e**)s obtained using the following BF_3 amount ($\times 10^{-2}$ molar amount) and solvent: (a) 8, toluene; (b) 8, a mixture of toluene and DCM (2 : 1 in a volume ratio); (c) 8, DCM; (d) 15, DCM; (e) 25, DCM. Figures at peak tops indicate molecular weights ($\times 10^{-4}$) estimated from those of polystyrene standards.

The endo- and exothermic peaks at lower temperatures than T_i are ascribed to other phase transitions. Some representative textures (A to G) taken by POM upon cooling are shown in Fig. 6. As shown by textures A and B, during the first cooling process of poly(**2c**), although a schlieren pattern was observed over the temperature range from 263 °C to room temperature, spots appeared faintly in the schlieren texture below 95 °C. Cooled from T_i, poly(**2i**) also showed a schlieren texture in which spots began to appear clearly around 190 °C, as exemplified by texture C; these spots increased so as to alter the schlieren pattern into a bunch-like type (texture D). The bunches quickly changed to broken fans at around 170 °C; this broken fan-shaped texture was observed over the temperature range from 170 °C to room temperature (texture E). Poly(**2j**) showed a thread-like texture over only a narrow temperature range of about 15 °C below T_i; a texture of broken fans, which banded during cooling, was then observed, as exemplified by textures F and G.

Figure 7 shows X-ray diffraction patterns of poly(**2b**), poly(**2i**), and poly(**2j**), which were obtained by cooling them to room temperature during the first cooling of the above POM procedure. From these results, obviously, texture B was identified to be the nematic mesophase; poly(**2b**) also showed a change in texture similar to that of poly(**2c**). Texture G of poly(**2j**), taken at 22 °C, was identified to be the smectic mesophase, and texture E, which was taken at 166 °C by POM for poly(**2i**), may also be ascribable to the smectic mesophase, since poly(**2i**) gave a texture resembling texture E at room temperature.

The DSC curves of poly(**2a**) are shown in Fig. 8. During the first cooling process, a thread-like texture appeared at 151 °C, probably due to the nematic mesophase, and soon changed to an isotropic phase-like texture, which did not indicate a completely darkened field on POM. This texture was observed up to 124 °C, and then changed to a fan-

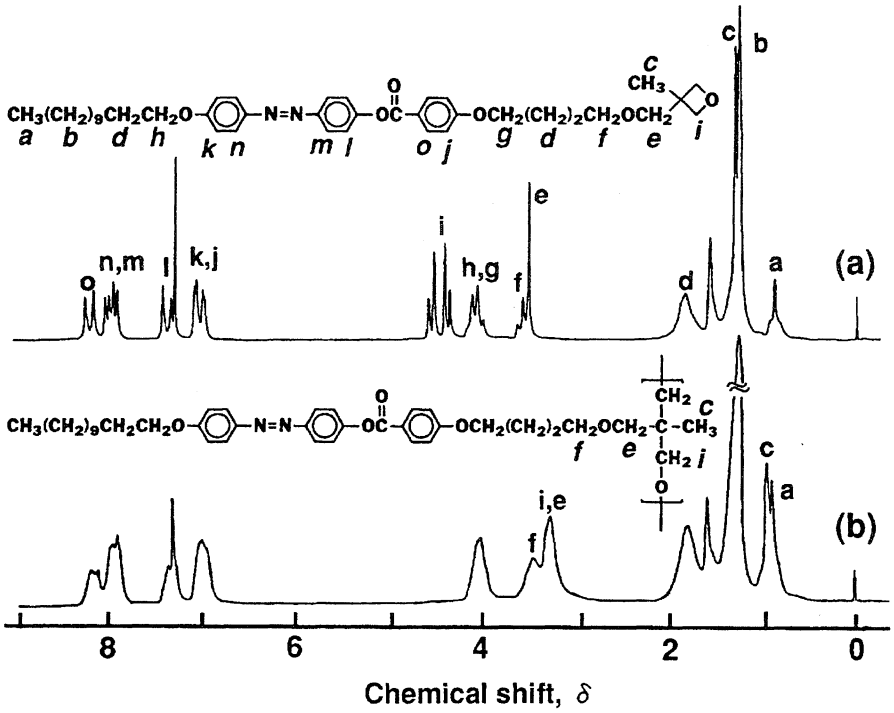

Fig. 3. ^{1}H NMR spectra of (a) **2k** and (b) poly(**2k**).

Table 2. Elemental Analysis Data of Polyoxetanes Poly-(**2a**)—Poly(**2k**)

	Anal (%)					
	Calcd			Found		
Polymer	C	H	N	C	H	N
Poly(**2a**)	70.87	6.37	5.90	70.72	6.41	5.92
Poly(**2b**)	69.03	6.39	5.55	68.44	6.34	5.92
Poly(**2c**)	69.48	6.61	5.40	69.66	6.72	5.41
Poly(**2d**)	69.91	6.81	5.26	69.65	6.81	5.19
Poly(**2e**)	70.31	7.01	5.12	70.02	6.97	5.07
Poly(**2f**)	70.69	7.19	5.00	70.44	7.13	5.03
Poly(**2g**)	71.06	7.37	4.87	70.88	7.52	4.85
Poly(**2h**)	71.40	7.53	4.76	71.14	7.64	4.70
Poly(**2i**)	71.73	7.69	4.65	71.30	7.80	4.61
Poly(**2j**)	71.80	8.14	4.53	72.17	8.11	4.38
Poly(**2k**)	72.92	8.26	4.25	72.67	8.20	4.29

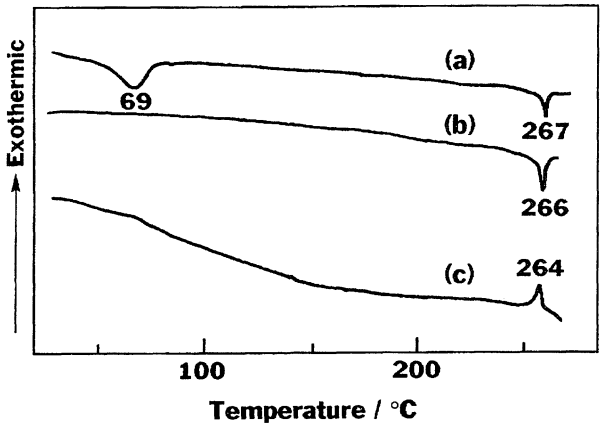

Fig. 4. DSC curves of poly(**2b**) on (a) 1st and (b) 2nd heating and (c) 1st cooling processes.

shaped texture, in which each fan seemed to be very small, via the appearance of spots at 124 °C in an isotropic phase-like texture. The change in the texture patterns of poly(**2a**) with cooling was similar to those of poly(**2d**) and poly(**2e**), rather than to those of poly(**2b**) and poly(**2c**). Figure 9 shows DSC curves during the first cooling process for the polymers obtained from **2e** with varying amounts of BF_3 in DCM or toluene. Poly(**2e**)-3 and poly(**2e**)-4, which had the fraction of lower M_{gpc} in higher content than poly(**2e**)-1 and poly(**2e**)-2, showed slightly lowered T_i values. The changes in the textures of the four poly(**2e**)s were scarcely different from each another, as observed by POM during the first cooling process. Their main mesophases are thought to be nematic based on the observation of a schlieren, or thread-like, texture in the temperature range from T_i to about 100 °C. These textures indicated the appearance of spots at around 90—100 °C, and then changed to a sand-like texture below this temperature. Thus, when M_{gpc} of the main fractions becomes around 10000, the thermal behavior of the pendant mesogens is hardly influenced by the MWD pattern of the main chain. The results of DSC measurements are summarized in Table 3 for poly(**2a**)—poly(**2k**) and in Table 4 for **2a**—**2k**.

The transition temperatures of the exothermic peaks on the first cooling process, furthermore, are plotted against the length of the tails in Fig. 10; a corresponding plot is shown in Fig. 11 for oxetanes **2a**—**2k**. As shown in Fig. 10, situation areas I—III were determined in order to classify the mesophases of polyoxetanes poly(**2a**)—poly(**2k**) based on their textures observed at appropriate temperatures by POM. In Fig. 10, poly(**2b**), poly(**2c**), and poly(**2d**), which have lower alkoxy groups as a tail, indicated the schlieren tex-

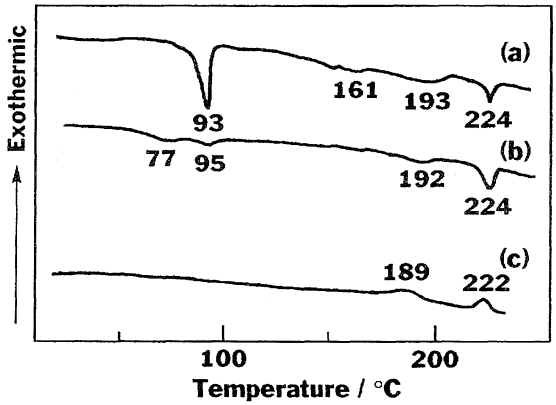

Fig. 5. DSC curves of poly(**2i**) on (a) 1st and (b) 2nd heating and (c) 1st cooling processes.

ture over the temperature range from 250 °C to about room temperature. As the tail is lengthened, the mesomorphic temperature range showing the schlieren texture becomes narrow, while the temperature range showing the broken fan-shaped texture is enlarged. As mentioned above for poly(**2e**)-1 to poly(**2e**)-4, poly(**2e**) with a moderately long tail of butoxy also showed bunch-like spots, which grew faintly in the schlieren texture, and soon changed to a sand-like texture. The appearance of bunches, however, was clearly observed for poly(**2f**)—poly(**2i**) with longer tails; such bunch-like textures changed to broken fan-shaped textures when just coming into situation area III, and poly(**2k**), with the longest tail of dodecyloxy, showed broken fan-shaped textures below T_i without any indication of the bunch-like texture. The fans of poly(**2f**)—poly(**2k**), moreover, became banded upon

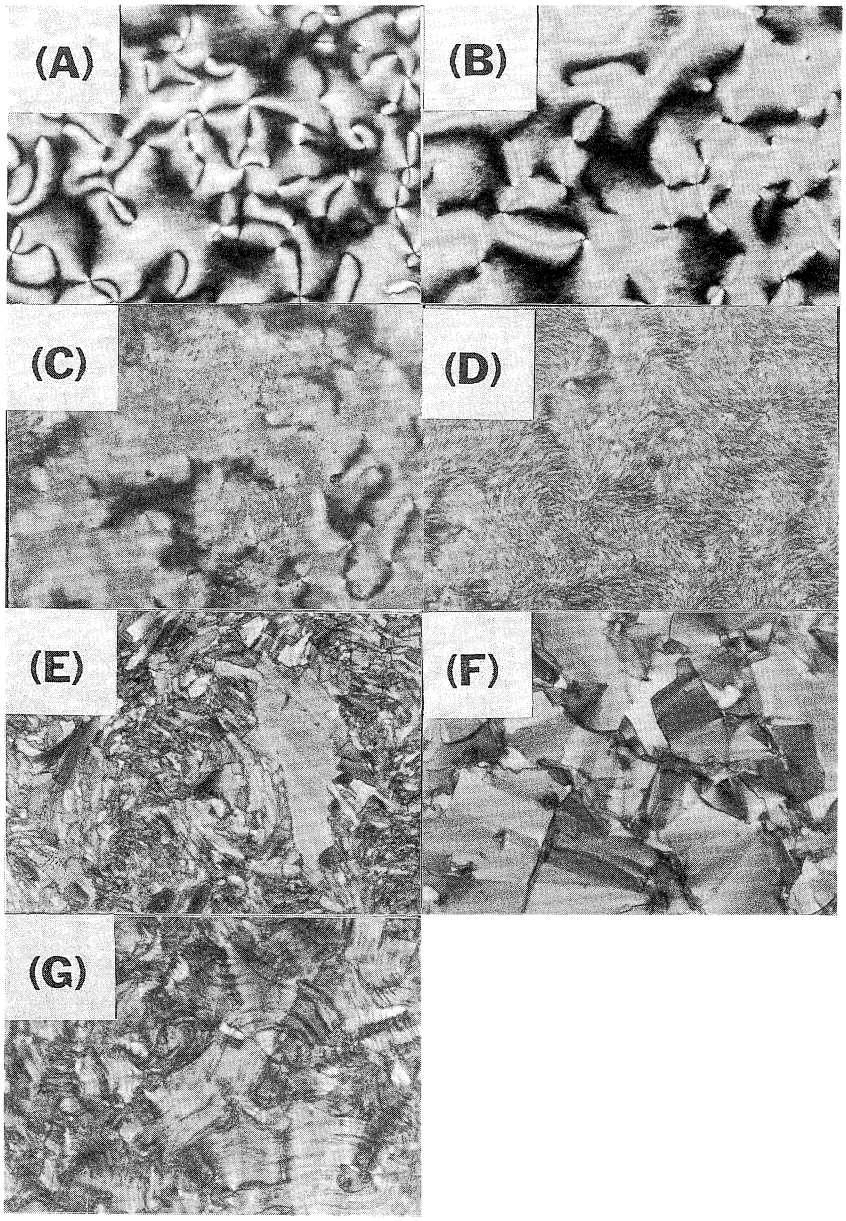

Fig. 6. Photomicrographs of poly(**2c**), poly(**2i**), and poly(**2j**) taken by POM at appropriate temperatures (magnification 200×). Poly(**2c**): (A) 207 and (B) 29 °C; poly(**2i**): (C) 190, (D) 180, and (E) 166 °C; poly(**2j**): (F) 209 and (G) 22 °C.

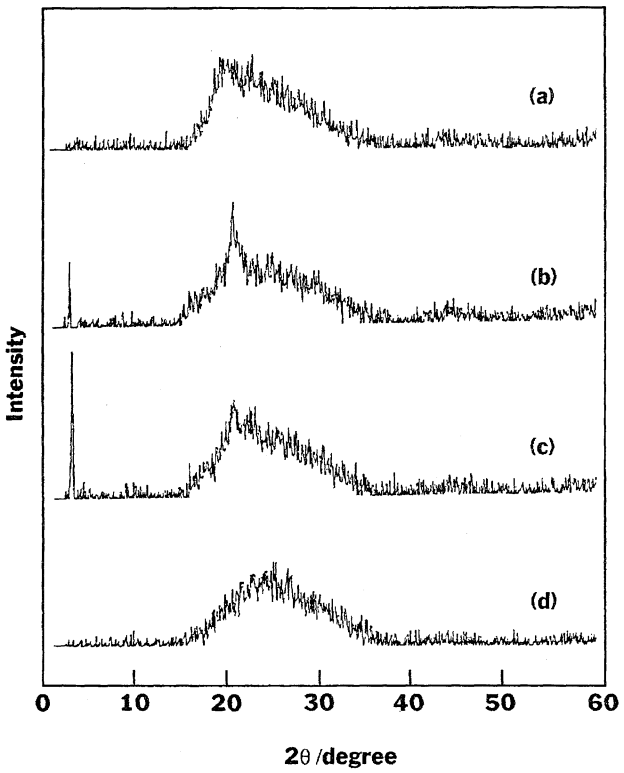

Fig. 7. X-Ray diffraction patterns of (a) poly(**2b**), (b) poly(**2i**), (c) poly(**2j**), and (d) a coverglass used to place these polymer samples.

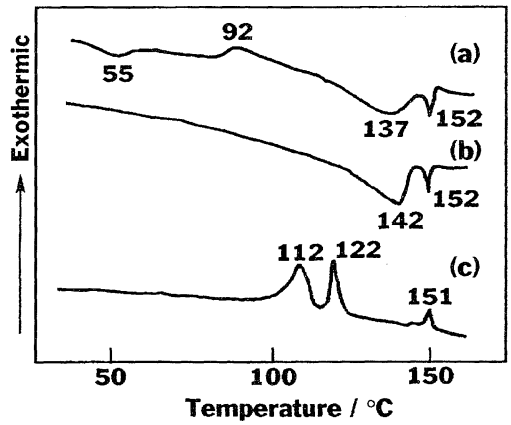

Fig. 8. DSC curves of poly(**2a**) on (a) 1st and (b) 2nd heating and (c) 1st cooling processes.

lowering the temperature of the polymer in the same way, as exemplified by texture G, although this transition peak could not be detected by DSC. When the bunch-like texture changed to the broken fan-shaped type, no DSC peak was observed, either. At this time, however, it is not clear whether such a change of the texture patterns can be ascribed to a phase transition. Concerning the change of the texture patterns, furthermore, the following is being considered. Since at a higher temperature range below T_i, the thermal motion of polymer matrices interferes with the growth of a mesophase layer, the mesophase layer is restricted to be formed in small domains, giving a bunch-like texture on POM. With a low-

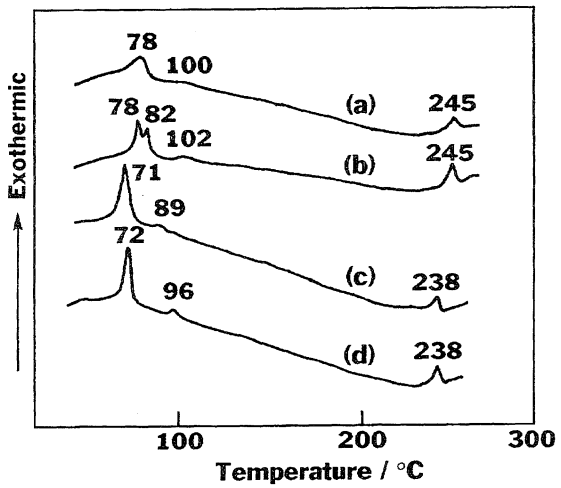

Fig. 9. DSC curves on 1st cooling process for (a) poly(**2e**)-1, (b) poly(**2e**)-2, (c) poly(**2e**)-3, and (d) poly(**2e**)-4.

ering of the temperature, however, an ordered assembly of the pendant mesogens is achieved in large domains due to increasing attractive interactions among the mesogens as well as due to a decreasing thermal-motion energy of the polymer matrices. Additionally, such an ordered assembly is favored by the van der Waals force of the long tails, such as OC_nH_{2n+1} ($n = 8$, 10, and 12) in poly(**2i**), poly(**2j**), and poly(**2k**), even in the higher temperature range below T_i. As exemplified by the DSC curve of poly(**2i**), and shown in the plot of Fig. 10, poly(**2d**)—poly(**2k**) indicated exothermic peaks in enthalpy of 1—4 J per g-polymer at temperatures of around 68 to 78 °C, at which point a distinct observation was not obtained by POM for the change to other mesophase textures. The exothermic peaks at these temperatures may be ascribable to the occurrence or change of the conformational structures in parts of the polyoxetane main chain, separated from the mesophase domains. Generally, three types of conformational structures are known for crystalline polyoxetane chains.[16,17] In this study, furthermore, it was difficult to clearly estimate the glass transition temperature (T_g) for the present polyoxetanes, although a slight change in the baseline of the DSC curve observed at around 20 to 30 °C may suggest the existence of T_g for these polyoxetanes.

On the other hand, poly(**1**)s having no benzoate moiety in the core of the mesogen also showed a texture due to a nematic mesophase over a very narrow temperature range upon cooling. When poly(**1e**) was cooled somewhat below the temperature at which the thread-like texture was observed, its polarized microphotograph showed the generation of spherulites in the thread-like texture, and then rapidly changed to a spherulitic texture. The thread-like textures of poly(**1b**) and poly(**1i**), which had a shorter or longer tail than poly(**1e**), also soon changed to their sand-like textures at the corresponding transition temperatures. The long alkoxy tails of poly(**1**)s, which have no benzoate moiety in the mesogenic core, were thus ineffective for the formation of well-grown mesophases. These findings therefore indicate the fact that the existence of the benzoate moiety in the mesogenic core

Table 3. Transition Temperatures of Polyoxetanes Poly(**2a**)—Poly(**2k**)

Polymers	Processes[a)]	Transition temperatures[b)]/°C
Poly(**2a**)	Heating	142(9.31), 152(0.64)
	Cooling	112(−6.72), 122(−2.73), 151(−0.68)
Poly(**2b**)	Heating	266(0.97)
	Cooling	264(−0.75)
Poly(**2c**)	Heating	33(0.28), 263(0.84)
	Cooling	263(−0.40)
Poly(**2d**)	Heating	87(3.65), 110(1.61), 250(0.77)
	Cooling	68(−3.32), 73(nd), 250(−0.50)
Poly(**2e**)	Heating	91(2.38), 107(nd), 120(nd), 248(1.87)
	Cooling	83(−2.71), 106(nd), 247(−0.96)
Poly(**2f**)	Heating	89(4.80), 113(nd), 138(0.85), 235(0.94)
	Cooling	77(−4.03), 110(nd), 134(−0.46), 235(−0.92)
Poly(**2g**)	Heating	79(1.78), 152(0.85), 231(1.02)
	Cooling	77(−1.81), 121(nd), 150(−0.62), 176(−0.47), 231(−0.68)
Poly(**2h**)	Heating	76(2.02), 169(2.21), 226(1.04)
	Cooling	76(−0.94), 170(−1.79), 225(−0.83)
Poly(**2i**)	Heating	77 and 95(2.25),[c)] 192(0.92), 224(1.19)
	Cooling	189(−2.54), 222(−1.45)
Poly(**2j**)	Heating	71(nd), 85(0.89), 208(2.86)
	Cooling	70(nd), 149(nd), 208(nd)
Poly(**2k**)	Heating	95(6.42), 221(7.76)
	Cooling	77 and 82(−4.68),[c)] 213(−2.40)

a) Second heating and 1st cooling. b) Figures in parentheses indicate enthalpy in J per g-polymer. The minus sign of enthalpy is given for exothermic peaks and nd for enthalpy not determined. c) Total enthalpy for overlapped peaks.

Table 4. Transition Temperatures of Oxetanes **2a**—**2k**

Monomers	Processes[a)]	Transition temperatures[b)]/°C
2a	Heating	102(24.18)
	Cooling	65 and 68(−20.16),[c)] 80(nd)
2b	Heating	41—55(nd),[d)] 70(25.44), 191(0.78)
	Cooling	190(−0.82)
2c	Heating	60(−4.14), 92(22.23), 203(0.936)
	Cooling	50(−13.35), 202(−1.01)
2d	Heating	68(nd), 80(17.20), 187(0.57)
	Cooling	50(−13.36), 185(−0.650)
2e	Heating	64(−2.35), 92(17.77), 188(0.636)
	Cooling	65(−14.36), 187(−1.01)
2f	Heating	81(−4.03), 93(21.50), 180(0.71)
	Cooling	75(−16.94), 179(−0.697)
2g	Heating	70(−3.61), 87(19.60), 179(0.787)
	Cooling	65(−13.90), 68(nd), 178(−0.77)
2h	Heating	54(−2.41), 89(23.14), 173(0.54)
	Cooling	69(−14.47), 172(−0.89)
2i	Heating	83(17.38), 171(0.78)
	Cooling	67(−14.48), 77(−0.67), 169(−0.83)
2j	Heating	48(−6.42), 89(18.09), 163(0.70)
	Cooling	65(−10.55), 92(−0.60), 162(−0.65)
2k	Heating	88(nd), 97(21.93), 105(nd), 157(0.60)
	Cooling	74(−18.36), 104(−0.75), 156(−0.68)

a) Second heating and 1st cooling. b) Figures in parentheses indicate enthalpy in J per g-polymer. The minus sign of enthalpy is given for exothermic peaks and nd for enthalpy not determined. c) Total enthalpy for overlapped peaks. d) Broad peak.

has an effect on maintaining the ordered assembly of pendant mesogens over a wide temperature range. Furthermore, when the benzoate moiety exists in the mesogenic core, the long alkoxy tails favor the formation of more highly ordered assemblies of the mesogens due to the van der Waals' attractive interaction of the tails.

As shown in Fig. 11, the profile of the plots for monomers **2a**—**2k** is different from that of their polymers. These monomers mainly indicated a schlieren texture due to the nematic mesophase, although a fan-shaped texture was also

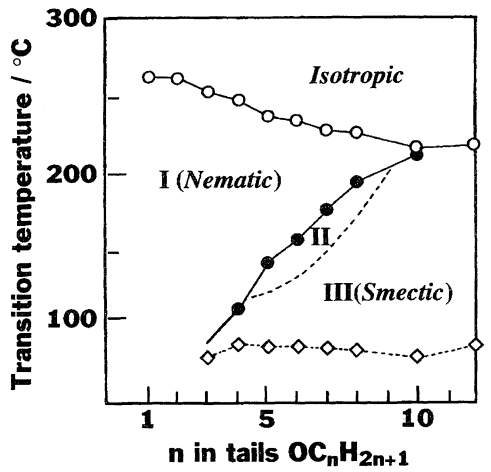

Fig. 10. Influence of the tail length of poly(**2b**)—poly(**2k**) on their transition temperatures and mesophases.

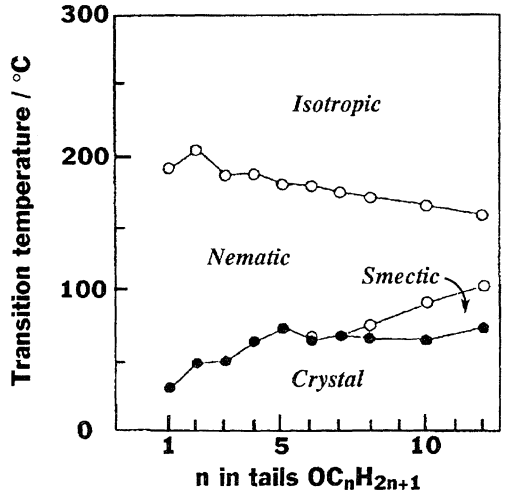

Fig. 11. Influence of the tail length of **2b**—**2k** on their transition temperatures and mesophases.

observed for monomers **2i**, **2j**, and **2k** with long tails, respectively, over narrow temperature ranges of 77—67, 92—65, and 104—74 °C. All of the monomers solidified at temperatures of around 50 to 70 °C, and the enthalpies at these temperatures were estimated to be about 10—20 J g^{-1}. From a comparison between the profiles in Figs. 10 and 11, it is suggested that the polyoxetane main chain also plays an important role to organize more highly ordered assemblies of the mesogenic groups. The pendant chains are linked to the quaternary carbon atoms of the main chain through the head methylene carbon atoms of the pendant chains, and the neighboring pendant chains are separated from each other by a 2-oxatrimethylene linkage, $-CH_2OCH_2-$. Therefore, such a polymer backbone favors a leveling of the pendant heads so as to organize a more highly ordered assembly of the pendant mesogens, such as a smectic mesophase, compared with those of the monomers not immobilized to the polymer chain.

As exemplified in the ^{1}H NMR spectrum for the aromatic ring of **2k** (Fig. 3), although protons H^k and H^j, located at the *o*-positions of the alkoxy groups in the tails and the spacer, resonate at $\delta = 6.94$—6.95, protons H^1, located at the *o*-position of the benzoyloxy group, resonate at $\delta = 7.32$. In general, these chemical-shift values were observed for the corresponding aromatic protons in a series of oxetanes **2b**—**2k** and their polymers. In **2a**, however, the *m*′-protons of the azobenzene ring showed multiplet signals at $\delta = 7.4$—7.6 together with the *p*′-proton in the same way as the *m*- and *p*-protons of azobenzene, which also resonate at $\delta = 7.4$—7.6. Thus, when the *p*-hydrogen atom of an azobenzene aromatic ring is replaced by an alkoxy group, the resultant *m*-hydrogen atoms resonate at a lower chemical shift by about 0.5 ppm than the original *m*-hydrogen atoms, indicating that the ether oxygen atom of the alkoxy groups has a positive mesomery effect on the resonance of the azobenzene aromatic ring. The *m*-hydrogen atoms (H^1) *ortho* to the benzoyloxy group, however, resonate at $\delta = 7.32$, which is an only slightly lowered chemical shift relative to $\delta = 7.4$—7.6 for the *m*′-hydrogen atoms of **2a**, indicating that the ether-like oxygen atom of an acyloxy group also faintly exerts such an effect. In fact, the alkoxy and acyloxy substituents are classified to the *o*- and *p*-orienting group in an electrophilic aromatic substitution. It is considered from these results that the coplanar resonance structure is not necessarily important between the benzoyloxy and azobenzene moieties. In the crystal structure of 4-butylphenyl 4-(4-butylbenzoyloxy)benzoate the torsion angle of the C–O bond next to the central phenyl ring was reported to be 60°.[18] Thus, the following structures are considered for the pendant mesogenic cores of poly(**2**)s and poly(**1**)s, as illustrated in Scheme 3. Although positively and negatively charged sites are formed in the azobenzene moiety of poly(**1**)s due to the mesomery effect of the alkoxy oxygen atoms of the spacer and tail segments, the vectors of these dipoles compensate each other. In the azobenzene moiety of poly(**2**)s, a dipole is generated between the electron-attractive azo group and the electron-releasing alkoxy oxygen atom of the tail, while the ether-like oxygen atom of the ester linkage scarcely exerts a mesomery

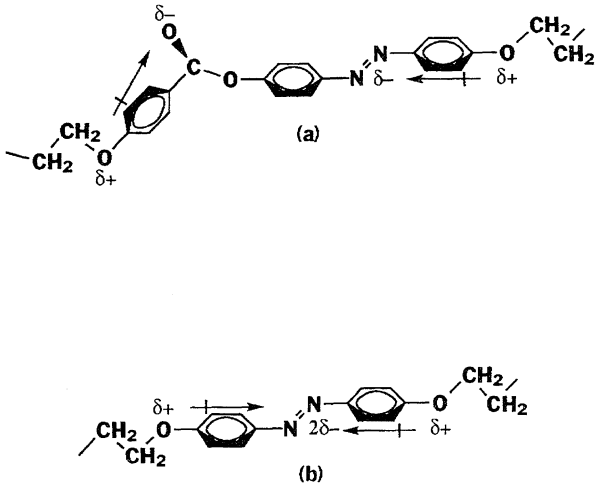

Scheme 3. The structures of mesogen cores considered for (a) poly(**2**)s and (b) poly(**1**)s.

effect. The benzoate moiety also has a dipole due to the formation of a positive charge in the alkoxy oxygen atom of the spacer and a negative charge in the carbonyl oxygen atom of the ester linkage. Presumably, these vectors, which do not compensate each other, play an important role to serve as a cohesive force of a dipole–dipole attractive interaction in the formation of stable mesophases; also the charged sites generated in the pendant mesogens may act, more or less, to produce π-electron donor–acceptor attractive interactions.

Contrary to the appearance of the mesophases of poly(**2**)s, polyoxetanes obtained from **3**—**6** did not show liquid-crystalline mesophases, as confirmed by DSC and POM. The reasons why the pendants of these polymers did not form any mesophases have not yet been clarified, although the following may be taken into account. The polarization of the ester carbonyl groups of poly(**3**) and poly(**4**) is not favored by the mesomery effect of the alkoxy oxygen atom located at the meta position of the benzoyl aromatic ring, and the methylene linkage of the phenyl acetate moiety in poly(**5**) interrupts the resonance between the ester carbonyl group and the spacer-linked phenoxy oxygen atom. Thus, the degrees of the carbonyl dipole moments of poly(**3**), poly(**4**), and poly(**5**) are inferior to those of poly(**2**)s. Poly(**6**) lacks the azobenzene moiety, which serves as a plate-like, polar segment.

In conclusion, the *p*-spacer-substituted benzoates containing an azobenzene moiety in the alcohol part of the ester were found to be good pendant mesogens based on the polyoxetane main chain. These polyoxetanes were readily obtained by the cationic ring-opening polymerization of the corresponding oxetane monomers with 0.08 molar amount of a $THF{\cdot}BF_3$ initiator. All of the polyoxetanes obtained in this study indicated liquid-crystalline properties showing several mesophases over a wide temperature range from about 250 °C to room temperature, as confirmed by DSC and POM, and by X-ray diffraction for the representatives of poly(**2**)s. It is thus known that the benzoate segment in poly(**2**)s is required to improve the liquid-crystalline quality to a remarkable extent, compared with that of poly(**1**)s. Although the corresponding monomers were also confirmed to be liquid-crystalline substances, their mesomorphic temperature ranges were narrower by 50 to 100 °C than those of the polyoxetanes. Moreover, highly ordered assemblies of mesogens could be achieved smoothly by immobilizing the mesogens to the polyoxetane chain. Thus, the main chains of the polyoxetanes may play an important role to support the liquid-crystalline ordering of their pendant mesogens through the spacers, presumably being affected by the physical and structural properties of the main chains, e.g., the flexibility, melt viscosity, polarity, and conformation of the main chains and a regular distance between the heads of the side chains. Such a role of the main chains of the side-chain liquid-crystalline polyoxetanes is becoming clear by comparing their liquid-crystalline properties with those of other flexible polymers, such as polyoxiranes and polysiloxanes, anchoring the mesogen and spacer comparable to those of the polyoxetanes, although appropriate samples must be prepared further for a comparison.

Experimental

Materials. Ethyl 4-[7-(3-Methyl-3-oxetanyl)-1,6-dioxaheptyl]benzoate (8): Obtained in a 90% yield by the reaction of bromide **7** (42 mmol) with an equimolar amount of ethyl 4-hydroxybenzoate in DMF (20 cm^3) at 80 °C for 15 h in the presence of powdered anhydrous K_2CO_3 (42 mmol): Bp 160—165 °C (8.0—9.3 Pa); IR (neat) 3080, 3060, 1600, 1580, 1470, and 850 (1,4-disubstituted benzene), 1710, 1280, and 1170 (ester), 1250 and 1035 (aromatic ether), 1110 (acyclic ether), and 980 and 840 cm^{-1} (cyclic ether); ^1H NMR ($CDCl_3$) $\delta = 1.30$—1.44 [total 6H: *s* ($\delta = 1.31$), CH_3 on the oxetane ring; *t* ($\delta = 1.37$), $J = 7.0$ Hz, $CO_2CH_2C\underline{H}_3$], 1.5—2.0 [4H, m, $OCH_2(C\underline{H}_2)CH_2O$], 3.48—3.60 [total 4H: *s* ($\delta = 3.48$), CH_2 adjacent to the oxetane ring; *t* ($\delta = 3.54$, $J = 5.7$ Hz), $OC\underline{H}_2(CH_2)_3OAr$], 3.98 (2H, *t*, $J = 5.9$ Hz, CH_2OAr), 4.34 (2H, *q*, $J = 7.1$ Hz, $CO_2C\underline{H}_2CH_3$), 4.35 and 4.51 (each 2H, AB-*q*, $J = 5.5$ Hz, CH_2 of the oxetane ring), 6.89 and 7.98 (each 2H, AB-*q*-like, $J = 9.0$ Hz, ArH).

4-[7-(3-Methyl-3-oxetanyl)-1,6-dioxaheptyl]benzoic Acid (9): Obtained in a 97% yield by heating the ester **8** (37 mmol) with 2 mol dm^{-3} NaOH (18 cm^3) in methanol (18 cm^3) under reflux: Mp 96—97 °C (ethyl acetate); IR (KBr) 3000—2400, 1670, and 1290 (COOH), 1245 (aromatic ether), 1015 (acyclic ether), 980 (cyclic ether), and 840 cm^{-1} (1,4-disubstituted benzene); ^1H NMR ($CDCl_3$) $\delta = 1.31$ (3H, *s*, CH_3), 1.6—2.1 [4H, *m*, $OCH_2(C\underline{H}_2)$-CH_2O], 3.4—3.6 [total 4H: *s* ($\delta = 3.48$) and *t* ($\delta = 3.59$, $J = 5.6$ Hz), $C\underline{H}_2OC\underline{H}_2(CH_2)_3O$], 4.04 (2H, *t*, $J = 5.9$ Hz, CH_2OAr), 4.35 and 4.51 (each 2H, AB-*q*, $J = 5.7$ Hz, CH_2 of the oxetane ring), and 6.89 and 8.01 (each 2H, AB-*q*-like, $J = 9.0$ Hz, ArH). The carboxylic proton was not detected, probably due to a broad signal.

4-(4-Dodecyloxyphenylazo)phenyl 4-[7-(3-Methyl-3-oxetanyl)-1,6-dioxaheptyl]benzoate (2k); Typical Procedure: The acid **9** (3.4 mmol) was stirred with 4-(4-dodecyloxyphenylazo)phenol (3.5 mmol) in DCM (20 cm^3) in the presence of DCC (3.5 mmol) and DMAP (0.4 mmol) at 0 °C for 2 h, and then at room temperature for another 2 h. After the ordinary post-treatment of the reaction mixture, the crude product was recrystallized from ethanol to give **2k** in an 80% yield: IR (KBr) 1740, 1270, and 1200 (ester), 1250 and 1070 (aromatic ether), 1120 (acyclic ether), 970 (cyclic ether), and 835 cm^{-1} (1,4-disubstituted benzene); ^1H NMR ($CDCl_3$) $\delta = 0.88$ [3H, *t*-like, $O(CH_2)_{11}C\underline{H}_3$], 1.1—1.6 [total 21H: *s* ($\delta = 1.31$), CH_3 of the oxetane ring; *m*, $O(CH_2)_2(C\underline{H}_2)_9CH_3$], 1.6—2.0 [total 6H: *m*, $OCH_2(C\underline{H}_2)_2CH_2O$ and $OCH_2C\underline{H}_2C_{10}H_{21}$], 3.4—3.7 [total 4H: *s* ($\delta = 3.49$), CH_2 adjacent to the oxetane ring; *t* ($\delta = 3.54$, $J = 6.1$ Hz), $OC\underline{H}_2(CH_2)_3OAr$], 3.9—4.2 [total 4H: *t* ($\delta = 4.03$, $J = 6.1$ Hz) and *t* ($\delta = 4.09$, $J = 6.1$ Hz), CH_2OAr], 4.35 and 4.50 (each 2H, AB-*q*, $J = 5.9$ Hz, CH_2 of the oxetane ring), and 6.9—8.3 [total 12H: AB-*q*-like ($\delta = 6.96$ and 7.88, $J = 8.8$ Hz), *m*′- and *o*′-ArHs of $N_2C_6H_4OC_{12}H_{25}$; AB-*q*-like ($\delta = 7.11$ and 8.26, $J = 8.8$ Hz), *m*- and *o*-ArHs of $OC_6H_4CO_2$); AB-*q*-like ($\delta = 7.32$ and 7.92, $J = 8.8$ Hz), *m*- and *o*-ArHs of $CO_2C_6H_4N_2$].

Found: C, 72.72; H, 8.06; N, 4.24%. Calcd for $C_{40}H_{54}N_2O_6$: C, 72.92; H, 8.26; N, 4.25%.

The other oxetanes, **2a**—**2j** and **3**—**6**, were obtained according to the preparation method of **2k** and recrystallized from ethanol.

4-(Phenylazo)phenyl 4-[7-(3-Methyl-3-oxetanyl)-1,6-dioxaheptyl]benzoate (2a): Yield 56%; IR (KBr) 1735, 1285, and 1230 (ester), 1255 and 1065 (aromatic ether), 1125 (acyclic ether), 975 (cyclic ether), and 840 cm^{-1} (1,4-disubstituted benzene); ^1H NMR ($CDCl_3$) $\delta = 1.31$ (3H, *s*, CH_3), 1.6—2.1 (4H, *m*), 3.4—3.7 [total 4H: *s* ($\delta = 3.49$); *t* ($\delta = 3.55$, $J = 5.8$ Hz)], 4.08 (total 4H: two triplets

superimposed no each other, $J=5.6$ Hz), 4.35 and 4.51 (each 2H, AB-*q*, $J=5.6$ Hz), and 6.9—8.3 [total 13H: AB-*q*-like ($\delta=6.96$ and 8.13, $J=8.9$ Hz), *m*- and *o*-ArHs of $OC_6H_4CO_2$; AB-*q*-like ($\delta=7.34$ and 7.97, $J=8.8$ Hz), *m*- and *o*-ArHs of $CO_2C_6H_4N_2$; *m* ($\delta=7.4$—7.6), *m*′- and *p*′-ArHs of $N_2C_6H_5$; *m* ($\delta=7.8$—8.0), *o*′-ArHs of $N_2C_6H_5$].

Found: C, 70.71; H, 6.27; N, 5.81%. Calcd for $C_{28}H_{30}N_2O_5$: C, 70.87; H, 6.37; N, 5.90%.

4-(4-Methoxyphenylazo)phenyl 4-[7-(3-Methyl-3-oxetanyl)-1,6-dioxaheptyl]benzoate (2b): Yield 86%; IR (KBr) 1720, 1270, and 1200 (ester), 1255 and 1070 (aromatic ether), 1110 (acyclic ether), 975 (cyclic ether), and 840 cm^{-1} (1,4-disubstituted benzene); ^1H NMR ($CDCl_3$) $\delta=1.31$ (3H, *s*, CH_3), 1.7—2.1 (4H, *m*), 3.4—3.7 [total 4H: *s* ($\delta=3.49$); *t* ($\delta=3.55$, $J=6.1$ Hz)], 3.88 (3H, *s*, OCH_3), 4.08 (2H, *t*, $J=5.7$ Hz), 4.34 and 4.50 (each 2H, AB-*q*, $J=5.7$ Hz), and 6.9—8.3 [total 12H: AB-*q*-like ($\delta=6.96$ and 7.89, $J=8.9$ Hz), *m*′- and *o*′-ArHs of $N_2C_6H_4OCH_3$; AB-*q*-like ($\delta=6.99$ and 8.13, $J=8.8$ Hz), *m*- and *o*-ArHs of $OC_6H_4CO_2$; AB-*q*-like ($\delta=7.32$ and 7.92, $J=8.8$ Hz), *m*- and *o*-ArHs of $CO_2C_6H_4N_2$].

Found: C, 68.63; H, 6.33; N, 5.35%. Calcd for $C_{29}H_{32}N_2O_6$: C, 69.03; H, 6.39; N, 5.55%.

4-(4-Ethoxyphenylazo)phenyl 4-[7-(3-Methyl-3-oxetanyl)-1,6-dioxaheptyl]benzoate (2c): Yield 63%; IR (KBr) 1730, 1270, and 1200 (ester), 1255 and 1060 (aromatic ether), 1115 (acyclic ether), 975 (cyclic ether), and 845 cm^{-1} (1,4-disubstituted benzene); ^1H NMR ($CDCl_3$) $\delta=1.32$ (3H, *s*), 1.46 (3H, *t*, $J=7.0$ Hz, $OCH_2C\underline{H}_3$), 1.7—2.1 (4H, *m*), 3.4—3.7 [total 4H: *s* ($\delta=3.48$); *t* ($\delta=3.55$, $J=6.0$ Hz)], 4.0—4.3 [total 4H: *t* ($\delta=4.07$, $J=6.7$ Hz); *t* ($\delta=4.11$, $J=7.0$ Hz)], 4.34 and 4.50 (each 2H, AB-*q*, $J=5.6$ Hz), and 6.9—8.3 [total 12H: AB-*q*-like ($\delta=6.95$ and 7.88, $J=8.9$ Hz); AB-*q*-like ($\delta=6.97$ and 8.12, $J=8.9$ Hz), AB-*q*-like ($\delta=7.32$ and 7.91, $J=8.8$ Hz)].

Found: C, 69.24; H, 6.60; N, 5.23%. Calcd for $C_{30}H_{34}N_2O_6$: C, 69.48; H, 6.61; N, 5.40%.

4-(4-Propoxyphenylazo)phenyl 4-[7-(3-Methyl-3-oxetanyl)-1,6-dioxaheptyl]benzoate (2d): Yield 83%; IR (KBr) 1730,1270, and 1200 (ester), 1255 and 1060 (aromatic ether), 1110 (acyclic ether), 975 (cyclic ether), and 840 cm^{-1} (1,4-disubstituted benzene); ^1H NMR ($CDCl_3$) $\delta=1.06$ (3H, *t*, $J=7.3$ Hz, $OCH_2CH_2C\underline{H}_3$), 1.31 (3H, *s*), 1.7—2.1 [total 6H: *m*, $OCH_2(C\underline{H}_2)_2CH_2O$ and $OCH_2C\underline{H}_2CH_3$], 3.4—3.7 [total 4H: *s* ($\delta=3.49$); *t* ($\delta=3.45$, $J=5.6$ Hz)], 3.9—4.2 [total 4H: *t* ($\delta=4.00$, $J=6.3$ Hz); *t* ($\delta=4.07$, $J=6.3$ Hz), $OC\underline{H}_2CH_2CH_3$], 4.35 and 4.51 (each 2H, AB-*q*, $J=5.6$ Hz), and 6.9—8.3 [total 12H: AB-*q*-like ($\delta=6.96$ and 7.88, $J=8.8$ Hz), AB-*q*-like ($\delta=6.98$ and 8.13, $J=8.9$ Hz), AB-*q*-like ($\delta=7.32$ and 7.92, $J=8.8$ Hz)].

Found: C, 70.16; H, 6.90; N, 5.16%. Calcd for $C_{31}H_{36}N_2O_6$: C, 69.91; H, 6.81; N, 5.26%.

4-(4-Butoxyphenylazo)phenyl 4-[7-(3-Methyl-3-oxetanyl)-1,6-dioxaheptyl]benzoate (2e): Yield 86%; IR (KBr) 1730, 1270, and 1200 (ester), 1255 and 1065 (aromatic ether), 1120 (acyclic ether), 970 (cyclic ether), and 845 cm^{-1} (1,4-disubstituted benzene); ^1H NMR ($CDCl_3$) $\delta=0.99$ [3H, *t*, $J=6.8$ Hz, $O(CH_2)_3C\underline{H}_3$], 1.31 (3H, *s*), 1.3—2.0 [total 8H: *m*, $OCH_2(C\underline{H}_2)_2CH_2O$ and $OCH_2(C\underline{H}_2)_2CH_3$], 3.4—3.7 [total 4H: *s* ($\delta=3.48$); *t* ($\delta=3.54$, $J=5.7$ Hz)], 3.9—4.2 [total 4H: *t* ($\delta=4.03$, $J=5.7$ Hz); *t* ($\delta=4.07$, $J=5.7$ Hz)], 4.34 and 4.50 (each 2H, AB-*q*, $J=5.7$ Hz), and 6.9—8.3 [total 12H: AB-*q*-like ($\delta=6.95$ and 7.87, $J=8.8$ Hz), AB-*q*-like ($\delta=6.94$ and 8.12, $J=8.9$ Hz), AB-*q*-like ($\delta=7.31$ and 7.92, $J=8.8$ Hz)].

Found: C, 70.22; H, 6.99; N, 4.97%. Calcd for $C_{32}H_{38}N_2O_6$: C, 70.31; H, 7.01; N, 5.12%.

4-(4-Pentyloxyphenylazo)phenyl 4-[7-(3-Methyl-3-oxetanyl)-1,6-dioxaheptyl]benzoate (2f): Yield 79%; IR (KBr) 1730, 1270, and 1200 (ester), 1255 and 1070 (aromatic ether), 1130 (acyclic ether), 990 (cyclic ether), and 840 cm^{-1} (1,4-disubstituted benzene); ^1H NMR ($CDCl_3$) $\delta=0.94$ [3H, *t*, $J=6.8$ Hz, $O(CH_2)_4C\underline{H}_3$], 1.31 (3H, *s*), 1.3—1.6 [4H, *m*, $O(CH_2)_2(C\underline{H}_2)_2CH_3$], 1.6—2.1 [total 6H: *m*, $OCH_2(C\underline{H}_2)_2CH_2O$ and $OCH_2C\underline{H}_2C_3H_7$], 3.4—3.7 [total 4H: *s* ($\delta=3.49$); *t* ($\delta=3.54$, $J=5.7$ Hz)], 3.9—4.2 [total 4H: *t* ($\delta=4.02$, $J=5.7$ Hz); *t* ($\delta=4.07$, $J=5.7$ Hz)], 4.42 and 4.58 (each 2H, AB-*q*, $J=5.8$ Hz), and 6.9—8.3 [total 12H: AB-*q*-like ($\delta=6.95$ and 7.88, $J=8.8$ Hz), AB-*q*-like ($\delta=6.97$ and 8.12, $J=9.0$ Hz), AB-*q*-like ($\delta=7.32$ and 7.92, $J=8.8$ Hz)].

Found: C, 70.45; H, 7.16; N, 5.05%. Calcd for $C_{33}H_{40}N_2O_6$: C, 70.69; H, 7.19; N, 5.00%.

4-(4-Hexyloxyphenylazo)phenyl 4-[7-(3-Methyl-3-oxetanyl)-1,6-dioxaheptyl]benzoate (2g): Yield 64%; IR (KBr) 1725, 1270, and 1200 (ester), 1255 and 1060 (aromatic ether), 1120 (acyclic ether), 980 (cyclic ether), and 840 cm^{-1} (1,4-disubstituted benzene); ^1H NMR ($CDCl_3$) $\delta=0.91$ [3H, *t*-like, $O(CH_2)_5C\underline{H}_3$], 1.2—1.6 [total 9H: *s* ($\delta=1.31$); *m*, $O(CH_2)_2(C\underline{H}_2)_3CH_3$], 1.6—2.1 [total 6H: *m*, $OCH_2(C\underline{H}_2)_2CH_2O$ and $OCH_2C\underline{H}_2C_4H_9$], 3.4—3.7 [total 4H: *s* ($\delta=3.49$); *t* ($\delta=3.55$, $J=5.9$ Hz)], 3.9—4.2 [total 4H: *t* ($\delta=4.03$, $J=5.7$ Hz); *t* ($\delta=4.07$, $J=5.7$ Hz)], 4.35 and 4.51 (each 2H, AB-*q*, $J=5.9$ Hz), and 6.9—8.2 [total 12H: AB-*q*-like ($\delta=6.95$ and 7.88, $J=8.9$ Hz), AB-*q*-like ($\delta=6.98$ and 8.13, $J=9.0$ Hz), AB-*q*-like ($\delta=7.32$ and 7.92, $J=8.8$ Hz)].

Found: C, 70.89; H, 7.42; N, 4.84%. Calcd for $C_{34}H_{42}N_2O_6$: C, 71.06; H, 7.37; N, 4.87%.

4-(4-Heptyloxyphenylazo)phenyl 4-[7-(3-Methyl-3-oxetanyl)-1,6-dioxaheptyl]benzoate (2h): Yield 80%; IR (KBr) 1725, 1265, and 1200 (ester), 1250 and 1055 (aromatic ether), 1120 (acyclic ether), 980 (cyclic ether), and 835 cm^{-1} (1,4-disubstituted benzene); ^1H NMR ($CDCl_3$) $\delta=0.90$ [3H, *t*-like, $O(CH_2)_6C\underline{H}_3$], 1.2—1.6 [total 11H: *s* ($\delta=1.31$); *m*, $O(CH_2)_2(C\underline{H}_2)_4CH_3$], 1.6—2.1 [total 6H: *m*, $OCH_2(C\underline{H}_2)_2CH_2O$ and $OCH_2C\underline{H}_2C_5H_{11}$], 3.4—3.7 [total 4H: *s* ($\delta=3.48$); *t* ($\delta=3.55$, $J=6.3$ Hz)], 3.9—4.2 [total 4H: *t* ($\delta=4.03$, $J=6.1$ Hz); *t* ($\delta=4.08$, $J=6.0$ Hz)], 4.35 and 4.51 (each 2H, AB-*q*, $J=5.5$ Hz), and 6.9—8.3 [total 12H: AB-*q*-like ($\delta=6.96$ and 7.88, $J=8.8$ Hz), AB-*q*-like ($\delta=7.11$ and 8.26, $J=8.9$ Hz), AB-*q*-like ($\delta=7.32$ and 7.92, $J=8.8$ Hz)].

Found: C, 71.15; H, 7.58; N, 4.65%. Calcd for $C_{35}H_{44}N_2O_6$: C, 71.40; H, 7.53; N, 4.76%.

4-(4-Octyloxyphenylazo)phenyl 4-[7-(3-Methyl-3-oxetanyl)-1,6-dioxaheptyl]benzoate (2i): Yield 73%; IR (KBr) 1730, 1270, and 1200 (ester), 1255 and 1060 (aromatic ether), 1120 (acyclic ether), 980 (cyclic ether), and 840 cm^{-1} (1,4-disubstituted benzene); ^1H NMR ($CDCl_3$) $\delta=0.89$ [3H, *t*-like, $O(CH_2)_7C\underline{H}_3$], 1.1—1.5 [total 13H: *s* ($\delta=1.31$); *m*, $O(CH_2)_2(C\underline{H}_2)_5CH_3$], 1.5—2.0 [total 6H: *m*, $OCH_2(C\underline{H}_2)_2CH_2O$ and $OCH_2C\underline{H}_2C_6H_{13}$], 3.4—3.6 [total 4H: *s* ($\delta=3.49$); *t* ($\delta=3.55$, $J=6.3$ Hz)], 3.9—4.2 [total 4H: *t* ($\delta=4.03$, $J=6.3$ Hz); *t* ($\delta=4.08$, $J=6.3$ Hz)], 4.35 and 4.50 (each 2H, AB-*q*, $J=5.7$ Hz), and 6.9—8.3 [total 12H: AB-*q*-like ($\delta=6.98$ and 7.87, $J=9.0$ Hz), AB-*q*-like ($\delta=6.98$ and 8.13, $J=8.9$ Hz), AB-*q*-like ($\delta=7.32$ and 7.92, $J=8.8$ Hz)].

Found: C, 71.69; H, 7.62; N, 4.68%. Calcd for $C_{36}H_{46}N_2O_6$: C, 71.73; H, 7.69; N, 4.65%.

4-(4-Decyloxyphenylazo)phenyl 4-[7-(3-Methyl-3-oxetanyl)-1,6-dioxaheptyl]benzoate (2j): Yield 80%; IR (KBr) 1740, 1270, and 1205 (ester), 1255 and 1075 (aromatic ether), 1120 (acyclic ether), 980 (cyclic ether), and 845 cm^{-1} (1,4-disubstituted benzene); ^1H NMR ($CDCl_3$) $\delta=0.88$ [3H, *t*-like, $O(CH_2)_9C\underline{H}_3$], 1.2—1.6 [total 17H: *s* ($\delta=1.32$); *m*, $O(CH_2)_2(C\underline{H}_2)_7CH_3$], 1.6—2.0 [total

6H: *m*, $OCH_2(C\underline{H}_2)_2CH_2O$ and $OCH_2C\underline{H}_2C_8H_{17}$], 3.4—3.7 [total 4H: *s* (δ = 3.49); *t* (δ = 3.55, *J* = 6.1 Hz)], 3.9—4.2 [total 4H: *t* (δ = 4.03, *J* = 6.1 Hz); *t* (δ = 4.08, *J* = 6.1 Hz)], 4.35 and 4.51 (each 2H, AB-*q*, *J* = 5.7 Hz), and 6.9—8.3 [total 12H: AB-*q*-like (δ = 6.96 and 7.88, *J* = 8.8 Hz), AB-*q*-like (δ = 6.98 and 8.13, *J* = 9.0 Hz), AB-*q*-like (δ = 7.32 and 7.92, *J* = 8.8 Hz)].

Found: C, 72.21; H, 7.89; N, 4.50%. Calcd for $C_{38}H_{50}N_2O_6$: C, 72.35; H, 7.99; N, 4.44%.

4-(4-Butoxyphenylazo)phenyl 3-[7-(3-Methyl-3-oxetanyl)-1,6-dioxaheptyl]benzoate (3): Yield 38%; IR (KBr) 1740, 1270, and 1200 (ester), 1250 and 1065 (aromatic ether), 1100 (acyclic ether), 980 (cyclic ether), an 835 and 745 cm^{-1} (1,4- and 1,3-disubstituted benzenes); ^1H NMR ($CDCl_3$) δ = 0.99 [3H, *t*, $O(CH_2)_3C\underline{H}_3$], 1.31 (3H, *s*, CH_3 of the oxetane ring), 1.4—1.7 [2H, *m*, $O(CH_2)_2C\underline{H}_2CH_3$], 1.7—2.1 [total 6H: *m*, $OCH_2(C\underline{H}_2)_2CH_2O$ and $OCH_2C\underline{H}_2C_2H_5$], 3.4—3.6 [total 4H: *s* (δ = 3.48), CH_2 adjacent to the oxetane ring; *t* (δ = 3.54, *J* = 5.5 Hz), $OC\underline{H}_2(CH_2)_3OAr$], 3.9—4.2 [total 4H: *t* (δ = 4.03, *J* = 6.1 Hz) and *t* (δ = 4.08, *J* = 6.1 Hz), CH_2OAr], 4.34 and 4.50 (each 2H, AB-*q*, *J* = 5.6 Hz, CH_2 of the oxetane ring), and 6.9—8.3 [total 12H: AB-*q*-like (δ = 6.98 and 7.88, *J* = 9.0 Hz), *m*′- and *o*′-ArHs of $N_2C_6H_4OC_4H_9$; AB-*q*-like (δ = 7.33 and 7.93, *J* = 8.9 Hz), *m*- and *o*-ArHs of $CO_2C_6H_4N_2$; *m*, ArHs of the benzoyl].

Found: C, 69.80; H, 6.74; N, 5.00%. Calcd for $C_{32}H_{38}N_2O_6$: C, 70.31; H, 7.01; N, 5.12%.

Bis[4-methoxyphenylazo)phenyl] 5-[7-(3-Methyl-3-oxetanyl)-1,6-dioxaheptyl]isophthalate (4): Yield 63%; IR (KBr) 1735, 1260, and 1195 (ester), 1220 and 1030 (aromatic ether), 1100 (acyclic ether), 980 (cyclic ether), and 835 and 745 cm^{-1} (1,4-di- and 1,3,5-trisubstituted benzenes); ^1H NMR ($CDCl_3$) δ = 1.32 (3H, *s*, CH_3 of the oxetane ring), 1.7—2.1 [4H, *m*, $OCH_2(C\underline{H}_2)_2CH_2O$], 3.4—3.7 [total 4H: *s*, (δ = 3.50), CH_2 adjacent to the oxetane ring; *t* (δ = 3.56, *J* = 6.1 Hz), $OC\underline{H}_2(CH_2)_3OAr$], 3.90 (6H, *s*, OCH_3), 4.15 (2H, *t*, *J* = 5.8 Hz, CH_2OAr), 4.34 and 4.50 (each 2H, AB-*q*, *J* = 5.7 Hz, CH_2 of the oxetane ring), 6.9—8.1 [total 18H: AB-*q*-like (δ = 6.99 and 7.90, *J* = 8.9 Hz), *m*′- and *o*′-ArHs of $N_2C_6H_4OCH_3$; AB-*q*-like (δ = 7.37 and 7.95, *J* = 8.9 Hz), *m*- and *o*-ArHs of $CO_2C_6H_4N_2$; *s*-like (δ = 7.97), 4- and 6-ArHs of the isophthaloyl], and 8.60 (1H, *s*-like, 2-ArH of the isophthaloyl).

Found: C, 67.70; H, 5.62; N, 7.14%. Calcd for $C_{43}H_{42}N_4O_9$: C, 68.06; H, 5.58; N, 7.38%.

4-(4-Butoxyphenylazo)phenyl 4-[7-(3-Methyl-3-oxetanyl)-1,6-dioxaheptyl]phenylacetate (5): Yield 55%; IR (KBr) 1760, 1270 (shoulder), and 1230 (ester), 1250 and 1065 (aromatic ether), 1130 (acyclic ether), 980 (cyclic ether), and 840 cm^{-1} (1,4-disubstituted benzene); ^1H NMR ($CDCl_3$) δ = 0.98 [3H, *t*, *J* = 6.8 Hz, $O(CH_2)_3C\underline{H}_3$], 1.31 (3H, *s*, CH_3 of the oxetane ring), 1.3—1.6 [2H, *m*, $O(CH_2)_2C\underline{H}_2CH_3$], 1.6—2.0 [total 6H: *m*, $OCH_2(C\underline{H}_2)_2CH_2O$ and $OCH_2C\underline{H}_2C_2H_5$], 3.4—3.7 [total 4H: *s* (δ = 3.47), CH_2 adjacent to the oxetane ring; *t* (δ = 3.52, *J* = 5.3 Hz), $OC\underline{H}_2(CH_2)_3OAr$], 3.80 (2H, *s*, $ArCH_2CO_2$), 3.9—4.2 [total 4H: *t* (δ = 3.98) and *t* (δ = 4.02), each *J* = 6.1 Hz, CH_2OAr], 4.34 and 4.50 (each 2H, AB-*q*, *J* = 5.7 Hz, CH_2 of the oxetane ring), and 6.7—8.0 [total 12H: AB-*q*-like (δ = 6.87 and 7.85, *J* = 8.9 Hz), *m*′- and *o*′-ArHs of $N_2C_6H_4OC_4H_9$; AB-*q*-like (δ = 6.97 and 7.15, *J* = 9.0 Hz), *m*- and *o*-ArHs of $OC_6H_4CH_2CO_2$; AB-*q*-like (δ = 7.27 and 7.85, *J* = 8.7 Hz), *m*- and *o*-ArHs of $CO_2C_6H_4N_2$].

Found: C, 70.23; H, 7.14; N, 4.74%. Calcd for $C_{33}H_{40}N_2O_6$: C, 70.70; H, 7.19; N, 5.00%.

4-Octyloxyphenyl 4-[7-(3-Methyl-3-oxetanyl)-1,6-dioxaheptyl]benzoate (6): Yield 77%; IR (KBr) 1720, 1275, and 1195 (ester), 1255 and 1075 (aromatic ether), 1115 (acyclic ether), 980 (cyclic ether), and 850 cm^{-1} (1,4-disubstituted benzene); ^1H NMR ($CDCl_3$) δ = 0.89 [3H, *t*-like, *J* = 6.8 Hz, $O(CH_2)_7C\underline{H}_3$], 1.2—1.6 [total 13H: *s* (δ = 1.31), CH_3 of the oxetane ring), *m*, $O(CH_2)_2(C\underline{H}_2)_5CH_3$], 1.6—2.1 [total 6H: *m*, $OCH_2(C\underline{H}_2)_2CH_2O$ and $OCH_2C\underline{H}_2C_6H_{13}$], 3.4—3.7 [total 4H: *s*, (δ = 3.48), CH_2 adjacent to the oxetane ring; *t* (δ = 3.54, *J* = 5.1 Hz), $OC\underline{H}_2(CH_2)_3OAr$], 3.9—4.2 [total 4H: *t* (δ = 3.98) and *t* (δ = 4.00), each *J* = 6.3 Hz, CH_2OAr], 4.34 and 4.50 (each 2H, AB-*q*, *J* = 5.7 Hz, CH_2 of the oxetane ring), and 6.8—8.3 [total 8H: AB-*q*-like (δ = 6.89 and 7.06, *J* = 9.2 Hz), *m*- and *o*-ArHs of $CO_2C_6H_4OC_8H_{17}$; AB-*q*-like (δ = 6.93 and 8.09, *J* = 8.8 Hz), *m*- and *o*-ArHs of $OC_6H_4CO_2$].

Found: C, 72.02; H, 8.64%. Calcd for $C_{30}H_{42}O_6$: C, 72.26; H, 8.49%.

4-(4-Alkoxyphenylazo)phenols: An aqueous solution of the diazonium chloride, prepared by the reaction of a 4-alkoxyaniline (40 mmol) in 4 mol dm^{-3} HCl (40 cm^3) with a 5.7 mol dm^{-3} aqueous solution of $NaNO_2$ (7 cm^3), was added at 0—3 °C to phenol (40 mmol) dissolved in a 10% aqueous NaOH solution (37 cm^3). The azo-coupling product was collected by filtration and recrystallized from benzene containing 10% hexane. The yields and melting points of the 4-alkoxy-substituted azobenzenes were as follows: Ethoxy: 83%, mp 123—124 °C; propoxy: 74%, mp 103—106 °C; butoxy: 83%, mp 84—86 °C; pentyloxy: 78%, 86—89 °C; hexyloxy: 55%, mp; 94—95 °C; heptyloxy: 62%, mp 100—102 °C; octyloxy: 61%, mp 84—86 °C; decyloxy: 53%, mp; 104—106 °C; dodecyloxy: 54%, mp 100—105 °C (recrystallized from benzene).

Polyoxetanes: A half of 1 g of an oxetane monomer was polymerized in DCM at 25—30 °C with 0.02—0.25 molar amount of $THF{\cdot}BF_3$. The product polymer was reprecipitated two or three times from DCM to methanol, and then dried in a vacuum.

Generally, poly(**2**)s showed the characteristic IR bands at the following wavenumbers: 1730, 1270, and 1200 (ester), 1260—1255 and 1060—1070 (aromatic ether), 1110—1100 (acyclic ether), and 840 cm^{-1} (1,4-disubstituted benzene) and poly(**2a**) indicated an additional band at 760 cm^{-1} (monosubstituted benzene). The ^1H NMR spectra of poly(**2**)s are shown in the following data.

Poly(2a): δ = 0.8—1.0 [3H, CH_3 adjacent to the quaternary carbon of the main chain (*s*-like signal centered at δ = 0.94)], 1.5—2.0 [4H, $OCH_2(C\underline{H}_2)_2CH_2O$], 3.1—3.6 [8H, CH_2 adjacent to the quaternary carbon and $OC\underline{H}_2(CH_2)_3OAr$], 3.9—4.2 (2H, CH_2OAr), 7.3—7.5 (2H, *m*-ArHs of $OC_6H_4CO_2$), 7.7—8.1 (5H, *m*-, *m*′-, and *p*′-ArHs of $CO_2C_6H_4N_2C_6H_5$), 8.3—8.5 (4H, *o*- and *o*′-ArHs of $CO_2C_6H_4N_2C_6H_5$), and 8.5—8.7 (2H, *o*-ArHs of $CO_6H_4CO_2$).

Poly(2b)s: δ = 0.8—1.0 (3H, *s*-like signal centered at δ = 0.93), 1.5—2.0 (4H), 3.1—3.6 (8H), 3.7—4.2 [5H, OCH_3 (*s*-like signal centered at δ = 0.94) and CH_2OAr], 6.8—7.1 (4H, *m*-ArHs of $OC_6H_4CO_2$ and *m*′-ArHs of $N_2C_6H_4OCH_3$), 7.1—7.4 (2H, *m*-ArHs of $CO_2C_6H_4N_2$), 7.8—8.1 (4H, *o*- and *o*′-ArHs of $C_6H_4N_2C_6H_4$), and 8.1—8.2 (2H, *o*-ArHs of the $OC_6H_4CO_2$).

Poly(2c): δ = 0.8—1.1 (3H, *s*-like signal centered at δ = 0.94), 1.2—1.5 [3H, $OCH_2C\underline{H}_3$ (*t*-like signal centered at δ = 1.44)], 1.5—2.0 (4H), 3.1—3.6 (8H), 3.9—4.2 (4H, CH_2OAr), 6.8—7.1 (4H), 7.1—7.4 (2H), 7.8—8.1 (4H), and 8.1—8.2 (2H).

Poly(2d): δ = 0.8—1.1 [6H, CH_3 (*s*-like signal centered at δ = 0.94) and $O(CH_2)_2C\underline{H}_3$ (*t*-like signal centered at δ = 1.04)], 1.5—2.0 [6H, $OCH_2(C\underline{H}_2)_2CH_2O$ and $OCH_2C\underline{H}_2CH_3$], 3.1—3.6 (8H), 3.9—4.2 (4H), 6.8—7.1 (4H), 7.1—7.4 (2H), 7.8—8.1 (4H), and 8.1—8.2 (2H).

Poly(2e)s: δ = 0.8—1.1 [6H, CH_3 (*s*-like signal centered at δ = 0.94) and $O(CH_2)_3C\underline{H}_3$ (*t*-like signal centered at δ = 0.97)], 1.5—2.0 [6H, $OCH_2(C\underline{H}_2)_2CH_2O$ and $OCH_2C\underline{H}_2C_2H_5$], 3.1—3.6

(8H), 3.9—4.2 (4H), 6.8—7.1 (4H), 7.1—7.4 (2H), 7.8—8.1 (4H), and 8.1—8.2 (2H).

Poly(2f): δ = 0.8—1.1 [6H, CH_3 adjacent to the quaternary carbon of the main chain and $O(CH_2)_4C\underline{H}_3$ (*s*- and *t*-like signal centered at δ = 0.94)], 1.3—1.5 [4H, $O(CH_2)_2(C\underline{H}_2)_2CH_3$], 1.5—2.0 [6H, $OCH_2(C\underline{H}_2)_2CH_2O$ and $OCH_2C\underline{H}_2C_3H_7$], 3.1—3.6 (8H), 3.9—4.2 (4H), 6.8—7.1 (4H), 7.1—7.4 (2H), 7.8—8.1 (4H), and 8.1—8.2 (2H).

Poly(2g): δ = 0.8—1.1 [6H, CH_3 adjacent to the quaternary carbon of the main chain and $O(CH_2)_5C\underline{H}_3$ (*s*- and *t*-like signal centered at δ = 0.93)], 1.3—1.5 [6H, $O(CH_2)_2(C\underline{H}_2)_3CH_3$], 1.5—2.0 [6H, $OCH_2(C\underline{H}_2)_2CH_2O$ and $OCH_2C\underline{H}_2C_4H_9$], 3.1—3.6 (8H), 3.9—4.2 (4H), 6.8—7.1 (4H), 7.1—7.4 (2H), 7.8—8.1 (4H), and 8.1—8.2 (2H).

Poly(2h): δ = 0.8—1.1 [6H, CH_3 (*s*-like signal centered at δ = 0.93) and $O(CH_2)_6C\underline{H}_3$ (*t*-like signal centered at δ = 0.89)], 1.3—1.5 [8H, $O(CH_2)_2(C\underline{H}_2)_4CH_3$], 1.5—2.0 [6H, $OCH_2(C\underline{H}_2)_2CH_2O$ and $OCH_2C\underline{H}_2C_5H_{11}$], 3.1—3.6 (8H), 3.9—4.2 (4H), 6.8—7.1 (4H), 7.1—7.4 (2H), 7.8—8.1 (4H), and 8.1—8.2 (2H).

Poly(2i): δ = 0.8—1.1 [6H, CH_3 (*s*-like signal centered at δ = 0.94) and $O(CH_2)_7C\underline{H}_3$ (*t*-like signal centered at δ = 0.88)], 1.3—1.5 [10H, $O(CH_2)_2(C\underline{H}_2)_5CH_3$], 1.5—2.0 [6H, $OCH_2(C\underline{H}_2)_2CH_2O$ and $OCH_2C\underline{H}_2C_6H_{13}$], 3.1—3.6 (8H), 3.9—4.2 (4H), 6.8—7.1 (4H), 7.1—7.4 (2H), 7.8—8.1 (4H), and 8.1—8.2 (2H).

Poly(2j): δ = 0.8—1.1 [6H, CH_3 (*s*-like signal centered at δ = 0.93) and $O(CH_2)_9C\underline{H}_3$ (*t*-like signal centered at δ = 0.88)], 1.3—1.5 [14H, $O(CH_2)_2(C\underline{H}_2)_7CH_3$], 1.5—2.0 [6H, $OCH_2(C\underline{H}_2)_2CH_2O$ and $OCH_2C\underline{H}_2C_8H_{17}$], 3.1—3.6 (8H), 3.9—4.2 (4H), 6.8—7.1 (4H), 7.1—7.4 (2H), 7.8—8.1 (4H), and 8.1—8.2 (2H).

Poly(2k): δ = 0.8—1.1 [6H, CH_3 (*s*-like signal centered at δ = 0.94) and $O(CH_2)_{11}C\underline{H}_3$ (*t*-like signal centered at δ = 0.88)], 1.3—1.5 [18H, $O(CH_2)_2(C\underline{H}_2)_9CH_3$], 1.5—2.0 [6H, $OCH_2(C\underline{H}_2)_2CH_2O$ and $OCH_2C\underline{H}_2C_{10}H_{21}$], 3.1—3.6 (8H), 3.9—4.2 (4H), 6.8—7.1 (4H), 7.1—7.4 (2H), 7.8—8.1 (4H), and 8.1—8.2 (2H). Also see Fig. 3 for the ^{1}H NMR spectrum of poly(**2k**).

The elemental-analysis data of the above polymers were given in Table 2.

The IR and ^{1}H NMR spectra of poly(**3**)—poly(**6**) were as follows:

Poly(3): IR (KBr) 1740, 1275, and 1200 (ester), 1255 and 1060 (aromatic ether), 1100 (acyclic ether), and 840 and 745 cm^{-1} (1, 3- and 1,4-disubstituted benzenes). ^{1}H NMR ($CDCl_3$) δ = 0.8—1.0 [6H, CH_3 adjacent to the quaternary carbon of the main chain (*s*-like signal centered at δ = 0.90) and $O(CH_2)_3C\underline{H}_3$ (*t*-like signal centered at δ = 0.98)], 1.3—2.0 [8H, $OCH_2(C\underline{H}_2)_2CH_2O$ and $OCH_2(C\underline{H}_2)_2CH_3$], 3.0—3.6 [8H, CH_2 adjacent to the quaternary carbon and $OC\underline{H}_2(CH_2)_3OAr$], 3.8—4.1 (4H, CH_2OAr), 6.9—8.3 (12H, *m*, ArHs).

Poly(4): IR (KBr) 1740, 1210, and 1190 (ester), 1255 and 1025 (aromatic ether), 1100 (acyclic ether), 840 and 745 cm^{-1} (1,4-di- and 1,3,5-trisubstituted benzenes). ^{1}H NMR ($CDCl_3$) δ = 0.8—1.0 (3H, CH_3 adjacent to the quaternary carbon of the main chain (*s*-like signal centered at δ = 0.91), 1.5—2.0 [4H, $OCH_2(C\underline{H}_2)_2CH_2O$] 3.0—3.6 [8H, CH_2 adjacent to the quaternary carbon and $OC\underline{H}_2(CH_2)_3OAr$], 3.8—4.2 [8H, OCH_3 (*s*-like signal centered at δ = 3.84) and CH_2OAr], 6.8—7.1 (4H, *m*′-ArHs of $N_2C_6H_4OCH_3$), 7.2—7.5 (4H, *m*-ArHs of $CO_2C_6H_4N_2$), 7.7—8.1, (10H, 4- and 6-ArHs of the isophthaloyl and *o*- and *o*′-ArHs of $C_6H_4N_2C_6H_4$), and 8.4—8.7 (1H, 2-ArH of the isophthaloyl).

Poly(5): IR (KBr) 1755, 1250, and 1150 (ester), 1250 (aromatic ether), 1120 (acyclic ether), and 840 cm^{-1} (1,4-disubstituted benzene). ^{1}H NMR ($CDCl_3$) δ = 0.8—1.1 [6H, CH_3 (*s*-like signal centered at δ = 0.92) and $O(CH_2)_3C\underline{H}_3$ (*t*-like signal centered at δ = 0.98)], 1.3—2.0 [8H, $OCH_2(C\underline{H}_2)_2CH_2O$ and $OCH_2(C\underline{H}_2)_2CH_3$], 3.6—4.1 [8H, CH_2 adjacent to the quaternary carbon and $OC\underline{H}_2(CH_2)_3OAr$], 3.8—4.2 [6H, $ArCH_2CO_2$ (*s*-like signal centered at δ = 3.77) and CH_2OAr], 6.7—7.4 (8H, ArHs of $OC_6H_4CH_2CO_2$ and *m*- and *m*′-ArHs of $C_6H_4N_2C_6H_4$), and 7.7—8.0 (4H, *o*- and *o*′-ArHs of $C_6H_4N_2C_6H_4$).

Poly(6): IR (KBr) 1735, 1280, and 1200 (ester), 1255 and 1075 (aromatic ether), 1105 (acyclic ether), and 845 cm^{-1} (1,4-disubstituted benzenes). ^{1}H NMR ($CDCl_3$) δ = 0.8—1.1 [6H, CH_3 (*s*-like signal centered at δ = 0.92) and $O(CH_2)_7C\underline{H}_3$ (*t*-like signal centered at δ = 0.89)], 1.3—1.5 [10H, $O(CH_2)_2(C\underline{H}_2)_5CH_3$], 1.5—2.0 [6H, $OCH_2(C\underline{H}_2)CH_2O$ and $OCH_2C\underline{H}_2C_6H_{13}$], 3.6—4.1 [8H, CH_2 adjacent to the quaternary carbon and $OC\underline{H}_2(CH_2)_3OAr$], 3.8—4.2 (4H, CH_2OAr), 6.8—7.2 (6H, ArHs of $CO_2C_6H_4OC_8H_{17}$ and *m*-ArHs of $OC_6H_4CO_2$), and 8.0—8.2 (2H, *o*-ArHs of $OC_6H_4CO_2$).

Measurement. IR and ^{1}H NMR spectroscopy, GPC, DSC, and POM were performed in the manner described in our previous report.[5] X-ray diffraction patterns were obtained by means of an X-ray diffraction apparatus (Rigaku Denki, RAD-RVC) using a Cu target under impression conditions of 3 kW (30 kV, 100 mA).

References

1) M. Motoi, S. Nagahara, H. Akiyama, M. Horiuchi, and H. Kanoh, *Polym. J.*, **21**, 987 (1989).

2) M. Motoi, E. Saito, S. Kyoda, N. Takahata, S. Nagai, and A. Arano, *Polym. J.*, **23**, 1225 (1991).

3) M. Motoi, S. Sekizawa, K. Asakura, and S. Kanoh, *Polym. J.*, **25**, 1283 (1993).

4) T. Hiruma, K. Kanoh, T. Yamamoto, S. Kanoh, and M. Motoi, *Polym. J.*, **27**, 78 (1995).

5) M. Motoi, K. Noguchi, A. Arano, S. Kanoh, and A. Ueyama, *Bull. Chem. Soc. Jpn.*, **66**, 1778 (1993).

6) Y. Kawakami, K. Takahashi, and H. Hibino, *Macromolecules*, **24**, 4531 (1991).

7) E. Akiyama, Y. Nagase, and N. Koide, *Makromol. Chem., Rapid Commun.*, **14**, 251 (1993).

8) Y. Lu and C. Hsu, *Macromolecules*, **28**, 1673 (1995).

9) Y. Kawakami, K. Takahashi, S. Nishiguchi, and K. Toida, *Polym. Int.*, **31**, 35 (1993).

10) S. Ujiie and K. Iimura, *Polym. J.*, **24**, 427 (1992).

11) M. Motoi, S. Nagahara, M. Yokoyama, E. Saito, O. Nishimura, S. Kanoh, and H. Suda, *Bull. Chem. Soc. Jpn.*, **62**, 1572 (1989).

12) E. J. Vandenberg, J. C. Mullis, and R. S. Juvet, Jr., *J. Polym. Sci., Part A: Polym. Chem. Ed.*, **27**, 3083 (1989).

13) E. J. Vandenverg, C. Mullis, R. S. Juvet, Jr., T. Miller, and R. A. Nieman, *J. Polym. Sci., Part A: Polym. Chem. Ed.*, **27**, 3113 (1989).

14) J. Kops, S. Hvilsted, and H. Spanggaard, *Macromolecules*, **13**, 1058 (1980).

15) E. Riande, J. G. de la Campa, J. Guzman, and J. de Abajo, *Macromolecules*, **17**, 1431 (1984).

16) H. Tadokoro, Y. Takahashi, Y. Chatani, and H. Kakida, *Makromol. Chem.*, **109**, 96 (1967).

17) H. Kakida, D. Makino, Y. Chatani, M. Kobayahsi, and H. Tadokoro, *Macromolecules*, **3**, 569 (1970).

18) P. Birner, S. Kugler, K. Simon, and G. Naray-Szabo, *Mol. Cryst. Liq. Cryst.*, **80**, 11 (1982).